

On the numerical integration of the Gross-Pitaevskii equation using Hermite-Fourier methods

Philipp Bader* and Sergio Blanes†

Universidad Politécnica de Valencia, Instituto de Matemática Multidisciplinar, E-46022 Valencia, Spain

We consider the numerical integration of the Gross-Pitaevskii equation with a potential trap given by a harmonic potential or a small perturbation to it. Splitting methods are frequently used with Fourier techniques since the system can be split into the kinetic and remaining part, and each part can be solved efficiently using Fast Fourier Transforms. To split the system into the quantum harmonic oscillator problem and the remaining part allows to get higher accuracies in many cases, but it requires to change between Hermite basis functions and the coordinate space. We show how to build new methods which combine the advantages of using Fourier methods while solving the harmonic oscillator exactly.

PACS numbers: 02.70.Hm

I. INTRODUCTION

We consider the numerical integration of the Gross-Pitaevskii equation (GPE)

$$i \frac{\partial}{\partial t} \psi(x, t) = \left(-\frac{1}{2\mu} \Delta + V(x) + \sigma |\psi(x, t)|^2 \right) \psi(x, t),$$

with $\sigma \in \mathbb{R}$ a constant and $V(x)$ the harmonic potential or a small perturbation to it, i.e. $V(x) = V_0(x) + V_I(x)$ with $V_0(x) = x^T M x$ (M being a symmetric positive definite matrix) and $V_I(x)$ is a small perturbation. This equation plays an essential role in the study of Bose-Einstein condensates. The non-linear term originates from the interaction between particles where the constant σ can be positive or negative for repulsive or attractive interactions [1, 2]. The numerical integration of the GPE has attracted great interest during the last years both for the computation of its ground state and its time evolution

[1, 2, 6, 7, 12, 14]. Several techniques have been analyzed: finite differences, Galerkin spectral methods, Fourier pseudospectral methods, pseudospectral methods with Hermite basis functions, etc. Among these methods, Fourier pseudospectral methods and methods with Hermite basis functions showed the highest performances for most problems [12]. Due to the nature of this problem, the wave function is trapped by the potential and vanishes asymptotically allowing us to consider it periodic when a sufficiently large spatial interval is assumed. Fourier pseudospectral methods can be implemented with Fast Fourier Transform (FFT) algorithms, achieving high accuracy with a moderate number of mesh points, and hence with relatively low computational cost. On the other hand, since $V(x)$ usually corresponds to a harmonic potential (or a small perturbation to it) whose solution can be written in terms of Hermite polynomials, it has been found that more accurate results can be

obtained if one solves separately the harmonic oscillator [2, 7, 12, 14].

In most cases, it is claimed that either the Hermite or the Fourier pseudospectral methods yield the most efficient schemes, the choice between the two depending on the particular parameter [12]. Motivated by these results, we combine both methods and rewrite them as a single simple pseudospectral Fourier scheme. This scheme gives the same accuracy as choosing the optimal number of Hermite basis functions, and avoids the transformation between the Hermite basis functions and the coordinate space.

From now on, for simplicity in the presentation, we consider the one-dimensional problem

$$i \frac{\partial}{\partial t} \psi = \left(-\frac{1}{2\mu} \frac{\partial^2}{\partial x^2} + \frac{1}{2} \mu \omega^2 x^2 + V_I(x) + \sigma |\psi(x, t)|^2 \right) \psi. \quad (\text{I.1})$$

The boundary conditions imposed by the trap require the wave function to go to zero at infinity, and up to any desired accuracy, we can assume $\psi(x, t)$ and all its derivatives, to vanish outside a finite region, say $x \in [a, b]$ which we split using a mesh (usually with $N = 2^k$ points to allow a simple use of the FFT algorithms). Then, the partial differential equation (I.1) transforms into a system of ordinary differential equations (ODEs)

$$i \frac{d}{dt} u(t) = \left(T + \frac{1}{2} \mu \omega^2 X^2 + V_I(X) + \sigma |u(t)|^2 \right) u(t), \quad (\text{I.2})$$

with $u \in \mathbb{C}^N$, where $u_i(t) \simeq \psi(x_i, t)$, $x_i = a + ih$, $h = (b - a)/N$, $X = \text{diag}\{x_0, \dots, x_{N-1}\}$ and T denotes a discretization of the kinetic part.

This system of non-linear ODEs can be numerically solved by standard methods for general ODEs. However, this problem has a very particular structure and for this reason the numerical methods can differ considerably both in the accuracy reached as well as in their computational costs. In addition, this problem has an important qualitative structure leading to the existence of several preserved quantities like the norm, energy, etc. The accurate preservation of these quantities as well as

* phiba@posgrado.upv.es

† serblaza@imm.upv.es

the error propagation associated to the methods allowed to conclude that splitting methods showed a high performance in most cases and are frequently the methods recommended for the time integration [2, 12, 14], making them the schemes considered in this work.

II. SPLITTING METHODS FOR THE TIME INTEGRATION

Let us consider the separable system of ODEs

$$u' = f^{[A]}(u) + f^{[B]}(u), \quad u(t_0) = u_0 \in \mathbb{C}^N, \quad (\text{II.1})$$

where we assume that both the systems

$$u' = f^{[A]}(u), \quad u' = f^{[B]}(u) \quad (\text{II.2})$$

can be either solved in closed form or accurately integrated. If $\varphi_t^{[A]}$, $\varphi_t^{[B]}$ represent the exact flows associated to (II.2) then, to advance the solution one time step, h , we can use, for example, the composition $\psi_h^{[1]} = \varphi_h^{[A]} \circ \varphi_h^{[B]}$ (i.e. $u(t_0 + h) \simeq \psi_h^{[1]}(u_0) = \varphi_h^{[A]}(\varphi_h^{[B]}(u_0))$) which corresponds to the well known first-order Lie-Trotter method. More efficient composition methods are obtained by its symmetrization

$$\psi_{h,A}^{[2]} = \varphi_{h/2}^{[A]} \circ \varphi_h^{[B]} \circ \varphi_{h/2}^{[A]} \quad (\text{II.3})$$

$$\psi_{h,B}^{[2]} = \varphi_{h/2}^{[B]} \circ \varphi_h^{[A]} \circ \varphi_{h/2}^{[B]} \quad (\text{II.4})$$

(referred as *ABA* and *BAB* compositions) which are second-order time-symmetric methods. In general, higher order methods can be obtained by the m -stage composition

$$\psi_h^{[p]} = \varphi_{a_m h}^{[A]} \circ \varphi_{b_m h}^{[B]} \circ \dots \circ \varphi_{a_1 h}^{[A]} \circ \varphi_{b_1 h}^{[B]} \quad (\text{II.5})$$

with appropriate coefficients $a_i, b_i \in \mathbb{R}$. If $a_m = 0$ or $b_1 = 0$ and $\psi_h^{[p]}$ is applied repeatedly, then the last map can be reused in the computations of the first map in the next step, and the schemes are considered as $(m - 1)$ -stage methods (First Same As Last, FSAL, property).

A method has order p if $\psi_h^{[p]} = \varphi_h + \mathcal{O}(h^{p+1})$ where φ_t denotes the exact global flow of (II.1). For linear problems, it is usual to replace the maps by exponentials (for non-linear problems we can also write the composition in terms of exponentials of Lie operators).

It is important to remark that, in general, most differential equations can be split in different ways. The computational cost of the schemes as well as the accuracy and the appropriate composition methods strongly depend on how the system has been split. For this reason, it is important to analyze the structure of the problem to decide the most appropriate split.

For our problem, the spatial derivative (or kinetic part) associated to the semidiscretized problem (I.2) can be solved in the momentum space by noting that

$$i \frac{d}{dt} u(t) = T u(t) = \mathcal{F}_N^{-1} D_N \mathcal{F}_N u, \quad (\text{II.6})$$

where D_N is diagonal and \mathcal{F}_N denotes the discrete Fourier transform of length N , whose computation can be accomplished by the FFT algorithm with $\mathcal{O}(N \log N)$ floating point operations. The solution of (II.6) for one time step, h , is given by

$$u(t+h) = \mathcal{F}_N^{-1} e^{-ihD_N} \mathcal{F}_N u(t)$$

which requires two FFT calls. The exponentials in e^{-ihD_N} need to be computed only once and can be reused at each step such that the cost of the action of e^{-ihD_N} corresponds to N complex products.

For the remaining part, the following well known result is very useful.

Lemma II.1 *The equation*

$$i \frac{\partial}{\partial t} \phi(x, t) = F(x, |\phi(x, t)|) \phi(x, t), \quad (\text{II.7})$$

$F: \mathbb{R}^n \times \mathbb{R} \rightarrow \mathbb{R}$, leaves the norm invariant, $|\phi(x, t)| = |\phi(x, 0)|$, and then

$$\phi(x, t) = e^{-itF(x, |\phi(x, 0)|)} \phi(x, 0). \quad (\text{II.8})$$

Proof. Taking the complex conjugate of (II.7) we get $-i\phi_t^* = F(x, |\phi|)\phi^*$ and with the product rule

$$\frac{d}{dt} |\phi|^2 = (-iF(x, |\phi|)\phi)\phi^* + \phi(iF(x, |\phi|)\phi^*) = 0,$$

the result $|\phi(x, t)| = |\phi(x, 0)|$ follows. Finally, the evolution of (II.7) is equivalent to the evolution of the following equation

$$i \frac{\partial}{\partial t} \phi(x, t) = F(x, |\phi(x, 0)|) \phi(x, t),$$

whose solution is given by (II.8). \square

On the other hand, it is well known that the solutions of the linear Schrödinger equation with the harmonic potential ($\mu = w = 1$)

$$i \frac{\partial}{\partial t} \phi(x, t) = \left(-\frac{1}{2} \frac{\partial^2}{\partial x^2} + \frac{1}{2} x^2 \right) \phi(x, t) \quad (\text{II.9})$$

can be expressed in terms of Hermite polynomials [9]:

$$\phi(x, t) = \sum_{n=0}^{\infty} c_n e^{-iE_n t} h_n(x) \quad (\text{II.10})$$

where

$$E_n = n + \frac{1}{2}, \quad h_n(x) = \frac{1}{\pi^{1/4} \sqrt{2^n n!}} H_n(x) e^{-x^2/2} \quad (\text{II.11})$$

and $H_n(x)$ are the Hermite polynomials satisfying the recursion

$$H_{k+1}(x) = 2xH_k(x) - 2kH_{k-1}, \quad k = 1, 2, \dots$$

and $H_0(x) = 1$, $H_1(x) = 2x$. The weights c_n can be computed from the initial conditions, $c_n = \langle h_n(x) | \phi(x, 0) \rangle$.

We can then split the system in two solvable parts, say

$$i\psi_t = (A + B)\psi \quad (\text{II.12})$$

and this can be done in different ways. We consider the following cases:

(i) Fourier(F)-split.

$$A = -\frac{1}{2} \frac{\partial^2}{\partial x^2}, \quad B = \frac{1}{2} x^2 + V_I(x) + \sigma |\psi|^2, \quad (\text{II.13})$$

which is the most frequently used split due to its simplicity. Here, A and B are diagonal in the momentum and coordinate spaces, respectively, and we can change between them using the Fourier Transform.

(ii) Harmonic oscillator(HO)-split.

$$A = -\frac{1}{2} \frac{\partial^2}{\partial x^2} + \frac{1}{2} x^2, \quad B = V_I(x) + \sigma |\psi|^2, \quad (\text{II.14})$$

where the solution for the equation $u' = Au$ can be approximated using a finite number of Hermite basis functions, i.e.

$$\phi_M(x, t) = \sum_{n=0}^{M-1} c_n e^{-iE_n t} h_n(x). \quad (\text{II.14b})$$

Since B is diagonal in the coordinate space it will act as a simple multiplication if we choose a number of Hermite basis functions and evaluate them at the points of a chosen mesh.

In both cases, we can use splitting methods to approximate the exact solution $\psi(x, t) = e^{-it(A+B)}\psi(x, 0)$, i.e. to approximate the operator $e^{-it(A+B)}$ by the composition (II.5) which, for convenience, we write as

$$\psi_h^{[p]} \equiv e^{-iha_m A} e^{-ihb_m B} \dots e^{-iha_1 A} e^{-ihb_1 B} \quad (\text{II.15})$$

with coefficients a_i, b_i such that $\psi_h^{[p]} = e^{-ih(A+B)} + \mathcal{O}(h^{p+1})$. Here, each exponential $e^{-iha_i A}$, $e^{-ihb_i B}$ stands for the exact flows of $i\psi_t = A\psi$ and $i\psi_t = B\psi$, respectively. One has to keep in mind that B depends on $|\psi|$ and it has to be updated at each stage because its value changes during the evolution of $e^{-iha_i A}$.

The simpler and faster procedure is to consider the split **(i)** because $A \equiv T$ can be computed in the momentum space, and one can easily and efficiently change from the momentum space to the coordinate space via FFTs. The choice **(ii)** allows us, however, to take advantage of the structure of the system, but it requires to solve the equation for the harmonic potential exactly (or with high accuracy). This can be done using Hermite polynomials (see [9, 12, 14]) and has its main advantage when, roughly speaking, $\|B\| < \|A\|$ since it allows us to use methods tailored for near-integrable systems which show

a high performance for this family of problems. The main drawback is that the evolution for $e^{-ih a_i A}$ has to be carried out using a basis of Hermite polynomials whereas the evolution for $e^{-ih b_i B}$ can be done either in space coordinates or using the basis of Hermite polynomials [9].

A. Solving the harmonic oscillator by Fourier methods

We propose a new method which combines the advantages of both splittings. It retains the accuracy of the HO-split **(ii)** while being as fast to compute as the F-split in **(i)**. The new scheme can be derived from the basic one-dimensional harmonic potential

$$i \frac{\partial}{\partial t} \psi(x, t) = \left(-\frac{1}{2} \frac{\partial^2}{\partial x^2} + \frac{1}{2} x^2 \right) \psi(x, t), \quad (\text{II.16})$$

in the following lemma where we denote $A_1 \equiv -\frac{1}{2} \frac{\partial^2}{\partial x^2}$, $B_1 \equiv \frac{1}{2} x^2$, so $e^{-ihA} \equiv e^{-ih(A_1+B_1)}$.

Lemma II.2 For $|h| < \pi$ the following property is satisfied

$$\begin{aligned} e^{-ih(A_1+B_1)} &= e^{-if(h)A_1} e^{-ig(h)B_1} e^{-if(h)A_1} \quad (\text{II.17}) \\ &= e^{-if(h)B_1} e^{-ig(h)A_1} e^{-if(h)B_1} \quad (\text{II.18}) \end{aligned}$$

where

$$g(h) = \sin(h), \quad f(h) = \tan\left(\frac{h}{2}\right). \quad (\text{II.19})$$

Proof. The algebraic structure of this problem is equivalent to the structure of the Hamiltonian for the one-dimensional classical harmonic oscillator, $H = \frac{1}{2}p^2 + \frac{1}{2}q^2$, with Hamilton equations

$$\frac{d}{dt} \begin{Bmatrix} q \\ p \end{Bmatrix} = \begin{pmatrix} 0 & 1 \\ -1 & 0 \end{pmatrix} \begin{Bmatrix} q \\ p \end{Bmatrix} = (A+B) \begin{Bmatrix} q \\ p \end{Bmatrix} \quad (\text{II.20})$$

with

$$A \equiv \begin{pmatrix} 0 & 1 \\ 0 & 0 \end{pmatrix}, \quad B \equiv \begin{pmatrix} 0 & 0 \\ -1 & 0 \end{pmatrix}. \quad (\text{II.21})$$

The Lie algebra generated by the matrices A, B is the same as the Lie algebra associated to the operators A_1, B_1 for the Schrödinger equation with the harmonic potential (II.16).

The exact evolution operator of (II.20) for one time step, h , is

$$O(h) = \begin{pmatrix} \cos(h) & \sin(h) \\ -\sin(h) & \cos(h) \end{pmatrix}, \quad (\text{II.22})$$

which is an orthogonal and symplectic 2×2 matrix. For the splitted parts, we have that

$$e^{f(h)A} = \begin{pmatrix} 1 & f(h) \\ 0 & 1 \end{pmatrix}, \quad e^{g(h)B} = \begin{pmatrix} 1 & 0 \\ -g(h) & 1 \end{pmatrix}$$

and then, equating the symmetric composition

$$e^{fA}e^{gB}e^{fA} = \begin{pmatrix} 1 - f \cdot g & 2f - f^2 \cdot g \\ -g & 1 - f \cdot g \end{pmatrix},$$

to (II.22), we obtain (II.19) which is valid for $h \neq k\pi$, $k \in \mathbb{Z} \setminus \{0\}$. Similarly, we have that

$$e^{fB}e^{gA}e^{fB} = \begin{pmatrix} 1 - f \cdot g & g \\ -2f + f^2 \cdot g & 1 - f \cdot g \end{pmatrix},$$

and equating to (II.22) yields the same result for $f(h), g(h)$ as given in (II.19) which holds, as before, for $|h| \neq k\pi$, $k \in \mathbb{Z} \setminus \{0\}$.

Both results remain valid, up to the first singularity at $h = \pi$, when replacing the 2×2 matrices by the corresponding linear operators A_1, B_1 . \square

REMARK 1: Notice that from (II.10) and (II.11), any wave function evolving under the harmonic potential (II.9) can be written as $\phi(x, t) = e^{-it/2}\varphi(x, t)$ with $\varphi(x, t + 2\pi) = \varphi(x, t)$, so $\phi(x, t + 2\pi) = -\phi(x, t)$, i.e. it is periodic with period 4π . However, the right hand sides of (II.17) and (II.18) are periodic with period 2π . For this reason, both approaches differ by a constant phase $e^{i\pi} = -1$ on the intervals $h \in [(2n-1)\pi, (2n+1)\pi]$, $n \in \mathbb{Z} \setminus \{0\}$ while being equivalent in the remaining intervals. Since a global phase has no physical meaning, one can extend the previous results from $h < \pi$ to $h \neq k\pi$, $k = \pm 1, \pm 2, \dots$

The result from the lemma was already obtained in a different way in [5], but the constraint $|h| < \pi$ was not analyzed.

REMARK 2: It is also important to keep in mind that the leap-frog methods (II.3) and (II.4), of second order in h , are stable for $h < 2$ (when applied to the harmonic oscillator (II.20)) and, in practice, the time step used is smaller.

It is immediate to generalize this result to the equation

$$i \frac{\partial}{\partial t} \psi(x, t) = \left(-\frac{1}{2\mu} \frac{\partial^2}{\partial x^2} + \mu \frac{w^2}{2} x^2 \right) \psi(x, t),$$

$\mu, w > 0$ by replacing (II.19) with

$$g = \frac{1}{\mu w} \sin(wh), \quad f = \mu w \tan\left(\frac{w}{2}h\right).$$

This result is valid for $|h| < h^* \equiv \pi/w$ (or for $|h| \neq h_k^* \equiv k\pi/w$ if we take Remark 1 into account).

III. THE HERMITE-FOURIER METHODS

Let us now solve the discretized GPE (I.2) by splitting methods using the symmetric compositions (II.3) and (II.4) with $A = A_1 + B_1$

$$\psi_{h,A}^{[2]} = e^{-ih(A_1+B_1)/2} e^{-ihB} e^{-ih(A_1+B_1)/2} \quad (\text{III.1})$$

$$\psi_{h,B}^{[2]} = e^{-ihB/2} e^{-ih(A_1+B_1)} e^{-ihB/2}. \quad (\text{III.2})$$

Notice that we can replace the exponentials $e^{\theta(A_1+B_1)}$ by (II.17) or (II.18) for the corresponding value of θ . There are four different possibilities and the computational costs differ considerably in each case. If one considers the FSAL property, both (III.1) and (III.2) are equivalent from the computational point of view and require one exponential of B and another one of A_1+B_1 per step. There is, however, a significant difference on using (II.3) with two kinetic terms which are the costly part of the scheme due to the FFT calls because the FSAL property is not fulfilled in this case[16]. If one uses (II.4) only one kinetic term is required. For example, the combination of (III.2) with (II.18) can be written as follows

$$\begin{aligned} \psi_h^{[2]} &= e^{-ihB/2} e^{-ih(A_1+B_1)} e^{-ihB/2} \\ &= e^{-ihB/2} e^{-if(h)B_1} e^{-ig(h)A_1} e^{-if(h)B_1} e^{-ihB/2} \\ &= e^{-i(hB/2+f(h)B_1)} e^{-ig(h)A_1} e^{-i(hB/2+f(h)B_1)} \end{aligned} \quad (\text{III.3})$$

which exactly solves the harmonic oscillator for $|h| < h^*$. This scheme only requires one kinetic term per step, and it gives the same accuracy as using a sufficiently large number of Hermite polynomials. The general composition (II.15) can be rewritten in the same way by replacing each flow $e^{-ia_i A}$ in (II.15) by the composition (II.18)

$$\begin{aligned} \Phi_h &\equiv e^{-i(hb_m B + \alpha_m B_1)} e^{-ig(a_m h)A_1} e^{-i(hb_m B + \alpha_{m-1} B_1)} \\ &\dots e^{-i(hb_1 B + \alpha_1 B_1)} e^{-ig(a_1 h)A_1} e^{-i\alpha_0 B_1} \end{aligned} \quad (\text{III.4})$$

where $\alpha_k = f(a_{k+1}h) + f(a_k h)$, $k = 0, 1, \dots, m+1$ with $a_0 = a_{m+1} = 0$. This method is valid for $|a_i h| < h^*$, $i = 1, \dots, m$, which only requires m calls of the FFT and its inverse, like the Fourier pseudospectral methods, but it reaches the same accuracy as if the Hermite functions were used.

There exist many different splitting methods in the literature which are addressed for different purposes, depending on the structure of the problem, the desired order, the required stability, etc. [3, 4, 8, 10, 11, 13, 15]. In the cases considered in (II.13) and (II.14), the operator A , containing the kinetic part, is quadratic in momenta and the operator B is diagonal in coordinate space. This fact allows us to use partitioned Runge-Kutta-Nyström methods. The coefficients for this family of methods have to solve a significantly reduced number of order conditions and, in general, their performance is superior to splitting methods designed for general separable problems. Efficient schemes of order 4 and 6 are obtained in [4]. On the other hand, we can consider the split (II.14) as a perturbation to the harmonic potential, i.e. $\|B\| \ll \|A\|$. If this is the case, we can find in the literature methods tailored for this class of problems which have shown a high performance in practice. Writing the equation (II.12) as $i\psi_t = (A + \epsilon B)\psi$ (with ϵ a small parameter), it is clear that the local error of the second order method (III.3) comes from the commutators at third order ($[A, [A, \epsilon B]]$ and $[\epsilon B, [A, \epsilon B]]$) and we can say that the local error is of order $\mathcal{O}(\epsilon h^3 + \epsilon^2 h^3)$. The coefficients

a_i, b_i in the general composition (III.4) can be chosen in order to cancel the dominant error terms, say, the $\mathcal{O}(\epsilon h^r)$ terms for relatively large values of r . Then, one can denote the effective order of a method by (r, p) with $r \geq p$ when the local error is given by $\mathcal{O}(\epsilon h^{r+1} + \epsilon^2 h^{p+1})$. The method is of order p , but in the limit $\epsilon \rightarrow 0$ it can be considered as of order $r \geq p$. Using this split allows to gain a factor ϵ in the accuracy even for general splitting methods where $r = p$. In [10] several methods of order $(r, 2)$ for $r \leq 10$ are obtained with all coefficients a_i, b_i positive. Furthermore, some other schemes of order $(r, 4)$ for $r = 6, 8$ are presented.

IV. NUMERICAL EXAMPLES

We analyze the performance of the methods considered in this work for the one-dimensional problem (I.1) with $\mu = w^2 = 1$, and the pure harmonic trap, i.e. $V_I = 0$.

To illustrate the validity of the decomposition presented in Lemma II.2 we first consider the linear problem ($\sigma = 0$). We take as the initial conditions the ground state at $t = 0$ whose exact solution is given by:

$$\psi(x, t) = \frac{1}{\pi^{1/4} \sqrt{2^n n!}} e^{-it/2} e^{-x^2/2}.$$

We consider $x \in [-10, 10]$, to ensure the wave function and its first derivatives vanish up to round off at the boundaries, and sample it at $N = 1024$ equidistant grid points. We integrate from $t = 0$ to T for $T \in [-2\pi, 4\pi]$, i.e. forward and backward in time. We measure the integrated error in the wave function, $\|u_{ex}(T) - u_a(T)\|_2$, where $u_a(T)$ denotes the approximate numerical solution obtained using the split (II.18) and $u_{ex}(T)$ denotes the exact solution at the discretized mesh. The result of this comparison is illustrated in Fig. 1 (left). The split (II.18) reproduces, for $|T| < \pi$, the exact solution up to round off, as expected. For $T \in [(2n-1)\pi, (2n+1)\pi]$, $n = 1, 2, \dots$, the complete loss of accuracy is due to the global phase mentioned in Remark 1. To illustrate this, in Fig. 1 (middle) we show the error $\| |u_{ex}(T)| - |u_a(T)| \|_2$ (where by $|u|$ we denote the vector whose components are the absolute value of the components of the vector u) and observe a perfect agreement away from the singularities. The right panel in Fig. 1 displays a zoom near a singularity where the error grows rapidly due to double precision arithmetic.

Let us now analyze how the approximation properties of the Hermite decomposition (II.14b) strongly depend on the function in question and on the chosen number of basis functions, M . We compute the M required to reach round-off precision for the evolution of a displaced ground state as initial condition, $\psi_\delta(x, 0) = e^{-(x-\delta)^2/2} / (\pi^{1/4} \sqrt{2^n n!})$ from $t = 0$ to $T = 10$ in one time step. If the initial conditions are computed on a mesh, this can be accomplished as follows [12]

$$u_{ex}(T) = e^{-iT(A_1+B_1)} u_0 \sim K^T e^{-iT D_1} K u_0 \quad (IV.1)$$

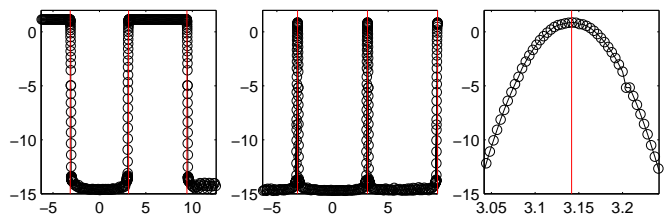


FIG. 1. Error in logarithmic scale for the integration of the ground state of the Harmonic potential using the split (II.18) for $T \in [-2\pi, 4\pi]$ (integration forward and backward in time). The left panel shows the 2-norm error, the middle panel the error when taking the absolute values of the components, and the right panel shows a zoom about $T = \pi$.

where $D_1 = \text{diag}\{\frac{1}{2}, \frac{3}{2}, \dots, \frac{2M-1}{2}\}$, M is the number of basis elements considered, and $K_{i,j} = h_{i-1}(x_j)$, $i = 1, \dots, M$, $j = 1, \dots, N = 512$ with $h_n(x)$ given in (II.10). We consider now $x \in [-10, 10]$. For $\delta = \frac{1}{10}$, round off accuracy is achieved with $M = 8$ while for $\delta = 2$ it is necessary to take $M = 29$. We observe that the Hermite decomposition is very sensitive to the initial conditions [9]. The Hermite basis works efficiently as far as the initial conditions as well as the evolution thereof can be accurately approximated using a few number of basis elements. In addition, for non-linear problems, the number of basis functions necessary to reach a given accuracy can vary along the time integration.

Next, we consider the following values for the parameter of the nonlinear term: $\sigma = 10^{-2}, 1, 10^2$. The cases $\sigma = 1$ and $\sigma = 10^2$ represent two moderately extreme cases of few and many particles in Bose-Einstein condensates [1, 2], and the case $\sigma = 10^{-2}$ illustrates the performance of the new methods if applied to problems (linear or non-linear) which are small perturbations of the Harmonic potential. We take in all cases the initial conditions $\psi(x, 0) = \rho e^{-(x-1)^2/2}$, with ρ a normalizing constant. We show in Fig. 2 the value of $|\psi(x, t)|^2$ at the initial and final time. The spatial interval is adjusted to ensure the wave function vanishes (up to round off) at the boundaries. We take $x \in [-20, 20]$ for $\sigma = 0.01$ and $x \in [-30, 30]$ for $\sigma = 1$ and $\sigma = 100$ where the wave function moves faster. One can appreciate that for strong nonlinearities the wave function can penetrate considerably on the potential barrier and one can expect that an accurate approximation of these wave functions requires a large number of Hermite functions when using (IV.1), making this procedure inappropriate.

A. HO-split versus F-split

We analyze now the advantage of considering the HO-split versus the F-split as given in (II.14) and (II.13). First, we consider the symmetric second order BAB leapfrog (LF) composition (III.2) where either the decomposition (II.18) or (IV.1) with several number of basis

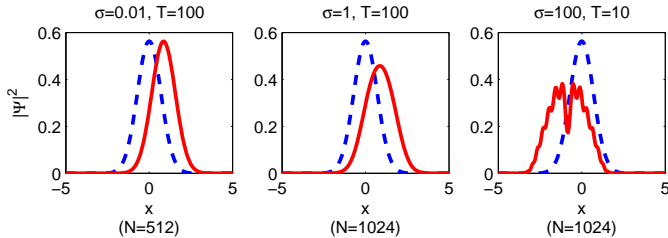


FIG. 2. Exact evolution at $t = T$ (solid line) from the initial conditions given by $\psi(x, 0) = \rho e^{-(x-1)^2/2}$ (dashed line). The number of grid points is given by N .

terms are considered for solving the harmonic potential. We take the same parameters, initial conditions and final times as in Fig. 2. Given a splitting method, say X , we denote by X_F , X_H and $X_H M$ its implementations with the F-split, the HO-split using the Hermite-Fourier method, and the HO-split using M Hermite basis functions in (IV.1). We measure the error versus the number of exponentials (which can be considered proportional to the computational cost). Figure 3 shows the results obtained for the three cases considered in Fig. 2. We can observe the improvement achieved by the HO-split. Using Hermite polynomials is advantageous when the perturbation is weak and the initial conditions can be accurately approximated by using a relatively few number of terms, but this number of terms should be increased in many cases along the time integration to keep a given accuracy. If the non linear part is strong many basis terms are necessary and the performance of the Hermite method significantly deteriorates. The Hermite-Fourier method proposed in this work (using the composition (II.18)) is clearly superior for weak perturbations and it keeps similar performance to the F-split for strong nonlinearities. At this point, we want to stress that fixing the number of Hermite basis functions bounds the maximally achievable accuracy and its limit depends on the initial condition and the strength of the nonlinearity.

Finally, we analyze the performance of different higher order splitting methods which are useful when high accuracies are desired. The following methods (whose coefficients are collected in Table I for convenience of the reader) are considered:

- RKN_64 (the 6-stage fourth-order method from [4]). This is a Partitioned Runge-Kutta-Nyström method and it is designed for the case where $[B, [B, [B, A]]] = 0$, being the case of both the F-split and the HO-split.
- $NI_4(8, 2)$ (the 4-stage (8,2) BAB method from [10]). This method is addressed for perturbed systems. One expects a high performance if the contribution from B is small.
- $NI_5(8, 4)$ (the 5-stage (8,4) BAB method from [10]).

We analyze in Figures 4-6 the three problems specified in Fig. 3. In the upper panels, the Leap-Frog methods, LF, are compared with the second order $NI_4(8, 2)$

TABLE I. Coefficients for several splitting methods.

The 6-stage 4th-order: $SRKN_64$	
$b_1 = 0.0829844064174052$	$a_1 = 0.245298957184271$
$b_2 = 0.396309801498368$	$a_2 = 0.604872665711080$
$b_3 = -0.0390563049223486$	$a_3 = 1/2 - (a_1 + a_2)$
$b_4 = 1 - 2(b_1 + b_2 + b_3)$	$a_4 = a_3, a_5 = a_2, a_6 = a_1$
$b_5 = b_3, b_6 = b_2, b_7 = b_1$	
The 4-stage (8,2) method: NI_4	
$b_1 = 1/20$	$a_1 = 1/2 - \sqrt{3/28}$
$b_2 = 49/18$	$a_2 = 1/2 - a_1$
$b_3 = 1 - 2(b_1 + b_2)$	$a_3 = a_2, a_4 = a_1$
$b_4 = b_2, b_5 = b_1$	
The 5-stage (8,4) method: NI_5	
$b_1 = 0.811862738544516$	$a_1 = -0.00758691311877447$
$b_2 = -0.677480399532169$	$a_2 = 0.317218277973169$
$b_3 = 1/2 - (b_1 + b_2)$	$a_3 = 1 - 2(a_1 + a_2)$
$b_4 = b_3, b_5 = b_2, b_6 = b_1$	$a_4 = a_2, a_5 = a_1$

methods. In the lower panels we compare the RKN_64 methods against the (8,4) methods jointly with the best among the previous second order methods.

For a weak non-linearity, when the system can be considered as a small perturbation to the harmonic potential, we clearly observe that the HO-split is superior to the F-split. In this case, with a relatively small number of Hermite functions, it is possible to approach accurately the solution, but this procedure has a limited accuracy which can deteriorate along the time integration and depends on the initial conditions. In addition, the methods addressed to perturbed problems show the best performance: The (8,2) $_H$ method shows the best performance when a relatively low accuracy is desired and the (8,4) $_H$ method does it for higher accuracies.

Figure 5 shows the results for $\sigma = 1$. It is qualitatively similar to the previous case yet the HO-split does not outperform the plain F-split (II.13) as significantly as before. Nevertheless, it is important to observe that, again, the best result is obtained for the HO decomposition. Notice that a higher number of Hermite basis functions is necessary to achieve the same accuracy as the Hermite-Fourier decomposition.

Finally, in Figure 6 we show the results for $\sigma = 100$. The HO-split cannot be expected to be particularly useful because the system is far from being close to a harmonic oscillator. From Fig. 2, we expect a great number of Hermite basis functions to be required for a sufficiently accurate expansion. The results in Figure 6 demonstrate this rather intuitive expectation, i.e. almost negligible precision in spite of the large number of basis terms $M = 150$. Remarkably, the proposed HO decomposition does not show these limitations and reaches the precision of the F-split (II.13) because we are solving the harmonic potential exactly up to spectral accuracy. For this prob-

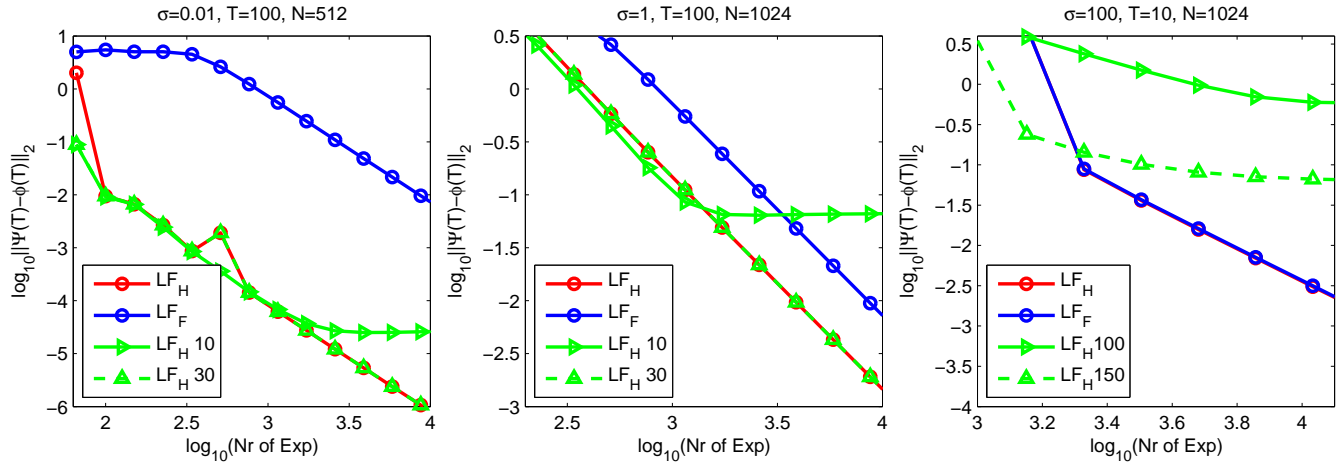


FIG. 3. Error versus the number of exponentials in logarithmic scale for different splittings for the Leap-Frog method.

lem, we observe that the (8,2) method has the best performance when a relatively low accuracy is desired, the (8,4) method shows the best performance for medium accuracies and the RKN_64 is the method of choice for higher accuracies.

V. CONCLUSIONS

Fourier methods have shown a high performance in solving many different problems which can be split into the kinetic part and a remaining part that is diagonal in the coordinate space. We have extended the Fourier methods to perturbations to the harmonic potential, and these methods are referred to as Hermite-Fourier methods. They solve exactly the linear Schrödinger equation with a harmonic potential (up to the accuracy given by the spatial discretization). These methods are fast to compute since they can be computed using FFTs and show a high accuracy when the problem is a small per-

turbation of the harmonic potential. The methods presented in this work extend to perturbations to the harmonic potential in linear quantum mechanics, and its performance is being analyzed at this moment, where it is straightforward to generalize the results to higher dimensions. The interesting case of explicitly time-dependent problems or the generalization of the decompositions (II.17) and (II.18) to the non-homogeneous case (i.e. $V_0(x) = x^T M x + G^T x$) is under investigation at this moment and the results will be published elsewhere.

ACKNOWLEDGMENTS

The authors acknowledge the support of the Generalitat Valenciana through the project GV/2009/032. The work of S. Blanes has also been partially supported by Ministerio de Ciencia e Innovación (Spain) under project MTM2007-61572 (co-financed by the ERDF of the European Union).

-
- [1] W. Bao, D. Jaksch, P. Markowich, Numerical solution of the Gross-Pitaevskii equation for Bose-Einstein condensation, *J. Comp. Phys.* **187** (2003) 318–342.
 - [2] W. Bao, J. Shen, A fourth-order time-splitting Laguerre-Hermite pseudospectral method for Bose-Einstein condensates, *SIAM J. Sci. Comput.* **26** (2005) 2010–2028.
 - [3] S. Blanes, F. Casas, and A. Murua, Splitting and composition methods in the numerical integration of differential equations, *Bol. Soc. Esp. Math. Apl.*, **45** (2008), 87–143.
 - [4] S. Blanes and P. C. Moan, Practical symplectic partitioned Runge-Kutta and Runge-Kutta-Nyström methods, *J. Comput. Appl. Math.*, **142** (2002), 313–330.
 - [5] S.A. Chin and E. Krotscheck, Fourth-order algorithm for solving the imaginary-time GrossPitaevskii equation in a rotating anisotropic trap, *Phys. Rev. E* **72** (2005), 036705.
 - [6] S.A. Chin, Dynamical multiple-time stepping methods for overcoming resonance instabilities, *J. Chem. Phys.* **120** (2004), 8–13.
 - [7] C.M. Dion, E. Cancés, Spectral method for the time-dependent Gross-Pitaevskii equation with a harmonic trap, *Phys. Rev. E* **67** (2003) 046706.
 - [8] E. Hairer, C. Lubich, and G. Wanner, *Geometric Numerical Integration. Structure-Preserving Algorithms for Ordinary Differential Equations*, Springer Ser. Comput. Math. 31, Springer-Verlag, Berlin (2002).
 - [9] C. Lubich, From quantum to classical molecular dynamics: reduced models and numerical analysis. Zurich Lectures in Advanced Mathematics. European Mathematical Society (EMS), Zürich, 2008.

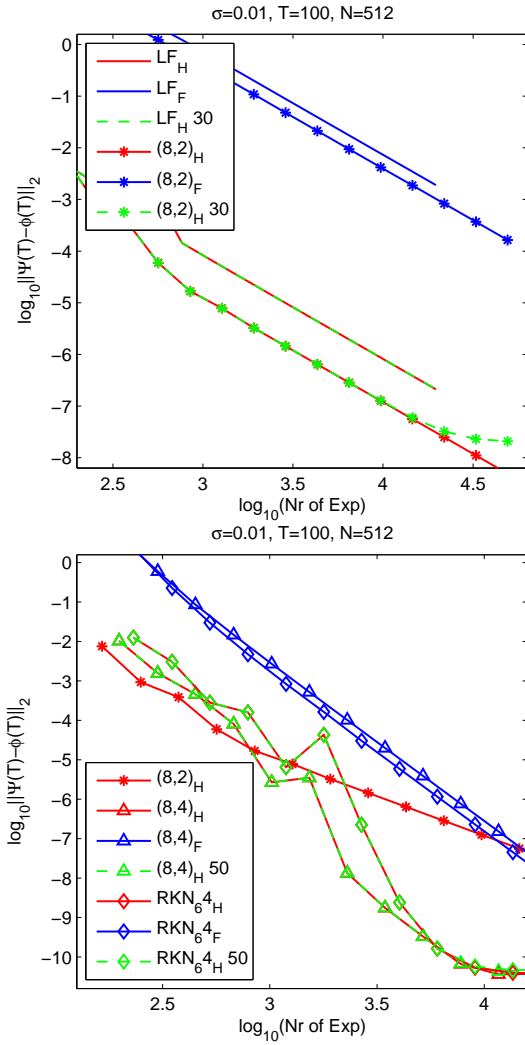


FIG. 4. Comparison of second order (upper panel) and fourth order (lower panel) methods for the different splittings and decompositions discussed in the text and $\sigma = 0.01$.

- [10] R. I. McLachlan, Composition methods in the presence of small parameters, *BIT*, **35** (1995), 258–268.
- [11] R.I. McLachlan and R. Quispel, Splitting methods, *Acta Numerica* **11** (2002), 341-434.
- [12] V.M. Pérez-García, X. Liu, Numerical methods for the simulation of trapped nonlinear Schrödinger systems, *Appl. Math. Comp.* **144** (2003) 215-235.

- [13] M. Suzuki, Fractal decomposition of exponential operators with applications to many-body theories and Monte Carlo simulations, *Phys. Lett. A* **146** (1990), 319–323.
- [14] M. Thalhammer, M. Caliani, and C. Neuhauser, High-order time-splitting Hermite and Fourier spectral methods, *J. Comput. Phys.* **228** (2009), 822–832.
- [15] H. Yoshida, Construction of higher order symplectic integrators, *Phys. Lett. A*, **150** (1990), 262–268.
- [16] More precisely, the computational costs are due to a change of coordinates realized by the Fourier transform which is for this type of problem equivalent to the num-

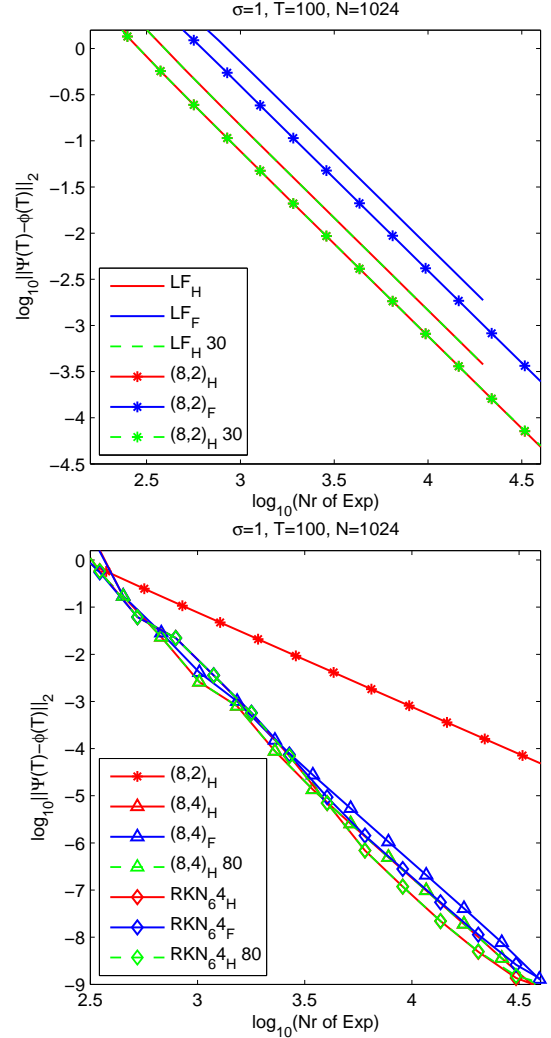


FIG. 5. Same as Fig. 4 for $\sigma = 1$.

ber of kinetic terms.

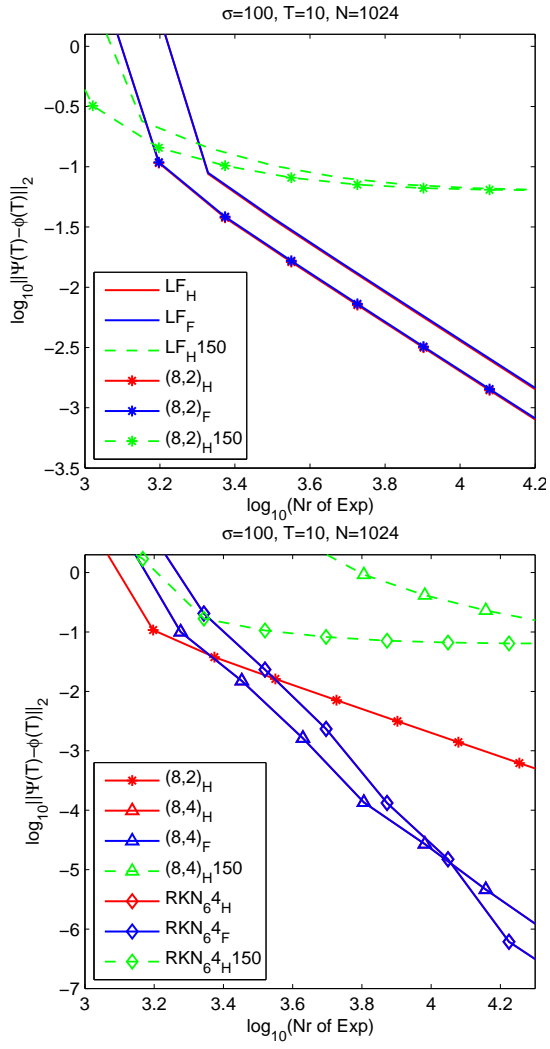


FIG. 6. Same as Fig. 4 for $\sigma = 100$. F-splittings overlap the corresponding Fourier-Hermite curves.